Supporting Information

Structurally Well-Defined Anion Conductive Aromatic Copolymers: Effect of the Side-Chain Length

Ryo Akiyama,[†] *Naoki Yokota,*[§], *Kanji Otsuji,*[‡] *and Kenji Miyatake**[*,†,‡]

[†] Fuel Cell Nanomaterials Center, and [‡] Clean Energy Research Center, University of Yamanashi, 4-4 Takeda, Kofu 400-8510, Japan

[§] Takahata Precision Co. Ltd., 390 Maemada, Sakaigawa, Fuefuki, Yamanashi, 406-0843, Japan

*Corresponding Author
E-mail miyatake@yamanashi.ac.jp; Tel +81 552208707; Fax +81 552208707 (KM).

General Method. ^{1}H NMR spectra were recorded on a JEOL JNM-ECA 500 (500 MHz) using $CDCl_3$, TCE-d_2 or DMSO-d_6 as a solvent and tetramethylsilane (TMS) as an internal reference. Chemical shifts are reported in ppm with TMS as the internal reference (δ 0.0). Data are reported as follows: chemical shift, multiplicity (s = singlet, d = doublet, t = triplet, q = quartet, m = multiplet, br = broad), coupling constants (Hz) and integration. ^{13}C NMR spectra were recorded on a JEOL JNM-ECA 500 (125 MHz) using $CDCl_3$ or DMSO-d_6 as a solvent with complete proton decoupling. Chemical shifts were recorded in ppm with the solvent references as the internal standard ($CDCl_3$: δ 77.0, DMSO-d_6: δ 39.5). Gel permeation chromatography (GPC) for oligomers was performed on a JASCO intelligent HPLC pump PU-2080 (flow rate = 0.5 mL min^{-1}) coupled with a photodiode array detector MD-2018, a column oven CO-2065 and a column Shodex SB-803HQ. GPC for polymers was performed on a JASCO intelligent HPLC pump PU-2080 (flow rate = 1.0 mL min^{-1}) coupled with an RI detector RI-2031, a multi-wavelength detector MD-2010, a column oven CO-965, and a column Shodex K-805L. In both measurements, DMF containing 0.01 M lithium bromide was used as eluent and column temperature was set at 50 °C. Molecular weight was calibrated with standard polystyrene samples. For transition electron microscopic (TEM) observation, the membranes were stained with tetrachloroplatinate ions by ion exchange of the ammonium groups in 0.5 M potassium tetrachloroplatinate (II) aqueous solution at 40 °C for 48 h, rinsed with deionized water, and dried at 60 °C under reduced pressure overnight. The stained membranes were embedded in epoxy resin, sectioned to 50 nm thickness with a Leica microtome Ultracut UCT, and placed on a copper grid. Images were taken on a Hitachi H-9500 TEM with an accelerating voltage of 200 kV. Hydroxide ion conductivity of the membranes was measured in degassed, deionized water using a four-probe conductivity cell attached to an AC impedance spectroscopy system (Solartron 1255B and 1287). Water uptake was measured at room temperature. Dynamic mechanical analysis (DMA) was carried out with an ITK DVA-225 dynamic viscoelastic analyzer. Temperature dependence of the storage moduli (E'), loss moduli (E''), and tan δ (E''/E') of QPE-*bl*-11 membranes in iodide ion forms was carried at 60% relative humidity (RH) and 10 Hz from room temperature to 95 °C at a heating rate of 1 °C min^{-1}.

All commercially available reagents were used as received for the reactions without any purification. For TLC analysis, Merk precoated TLC aluminum sheets (silica gel 60 F_{254}) were used. For preparative column

chromatography, Kanto Chemical Co., Inc. silica gel 60 N (spherical neutral, particle size 100–210 μm) and aluminium oxide (activated) were used.

Synthesis of Dichloromonomers 5 and 9.

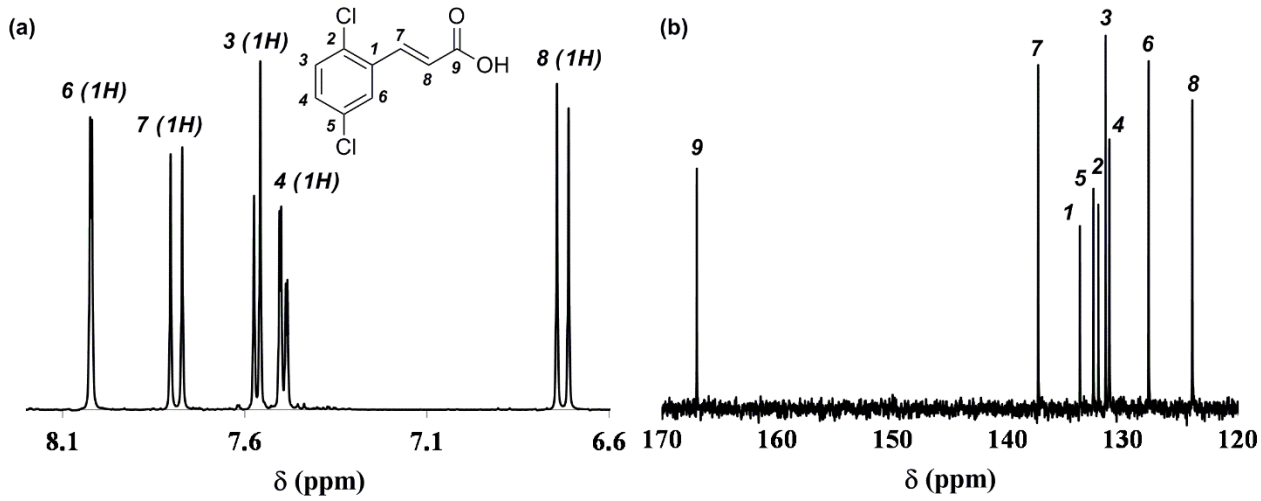

Figure S1. (a) ^{1}H and (b) ^{13}C NMR spectra of 2,5-dichlorocinnamic acid (**2a**) in DMSO-d_6.

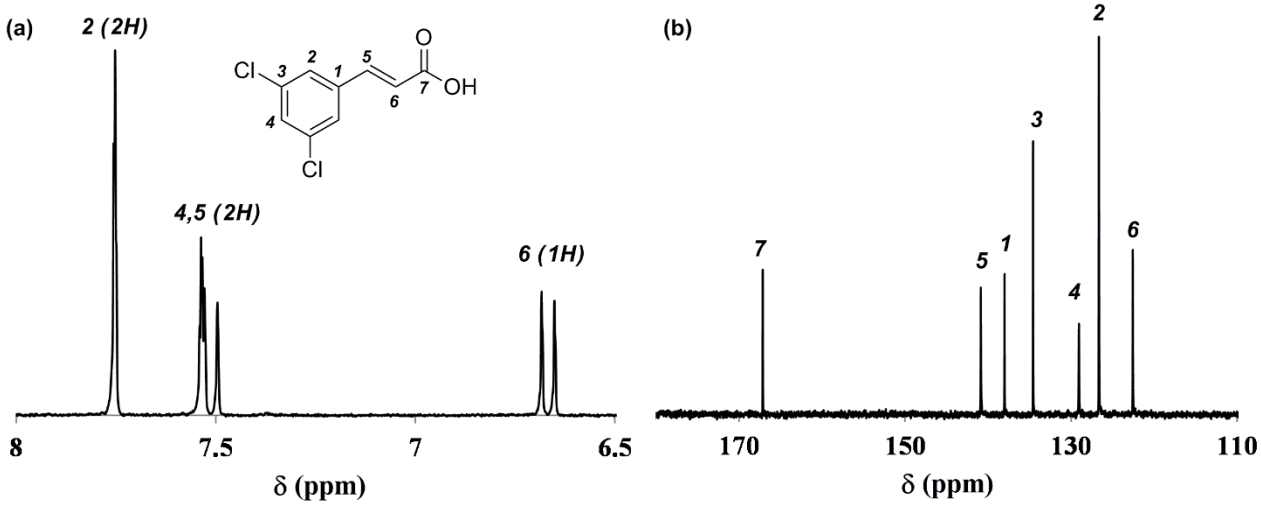

Figure S2. (a) ^{1}H and (b) ^{13}C NMR spectra of 3,5-dichlorocinnamic acid (**2b**) in DMSO-d_6.

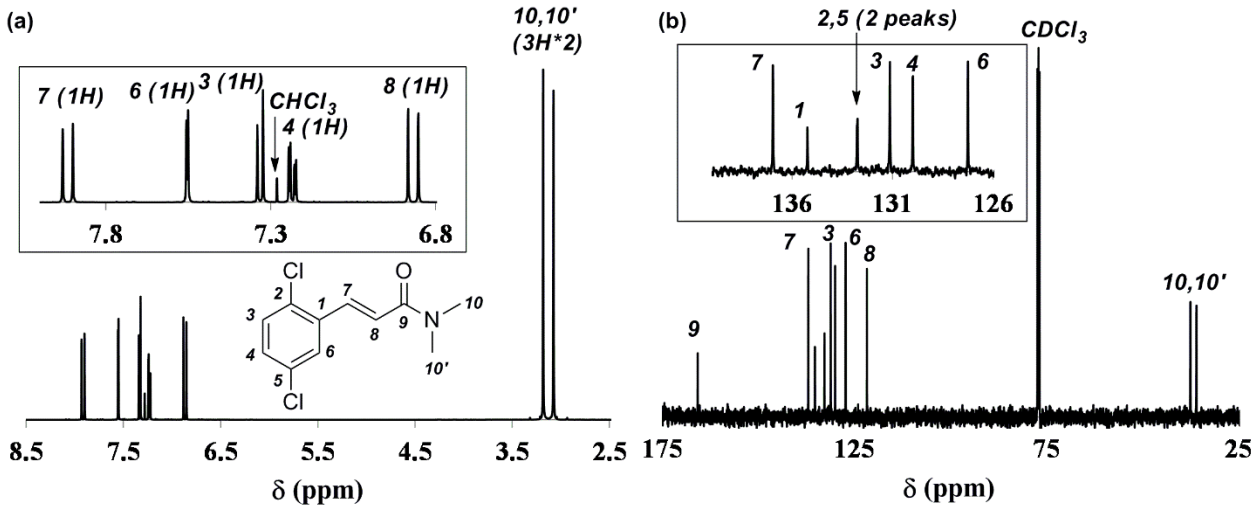

Figure S3. (a) ^{1}H and (b) ^{13}C NMR spectra of 3-(2,5-dichlorophenyl)-*N*,*N*-dimethyl-2-propenamide (**3a**) in $CDCl_3$.

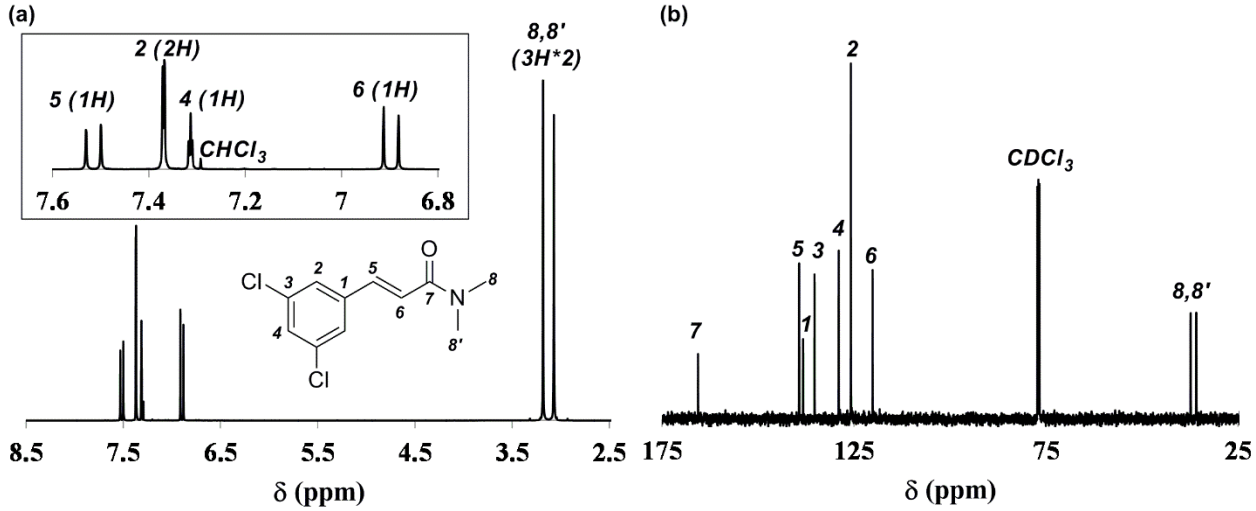

Figure S4. (a) ^{1}H and (b) ^{13}C NMR spectra of 3-(3,5-dichlorophenyl)-*N*,*N*-dimethyl-2-propenamide (**3b**) in $CDCl_3$.

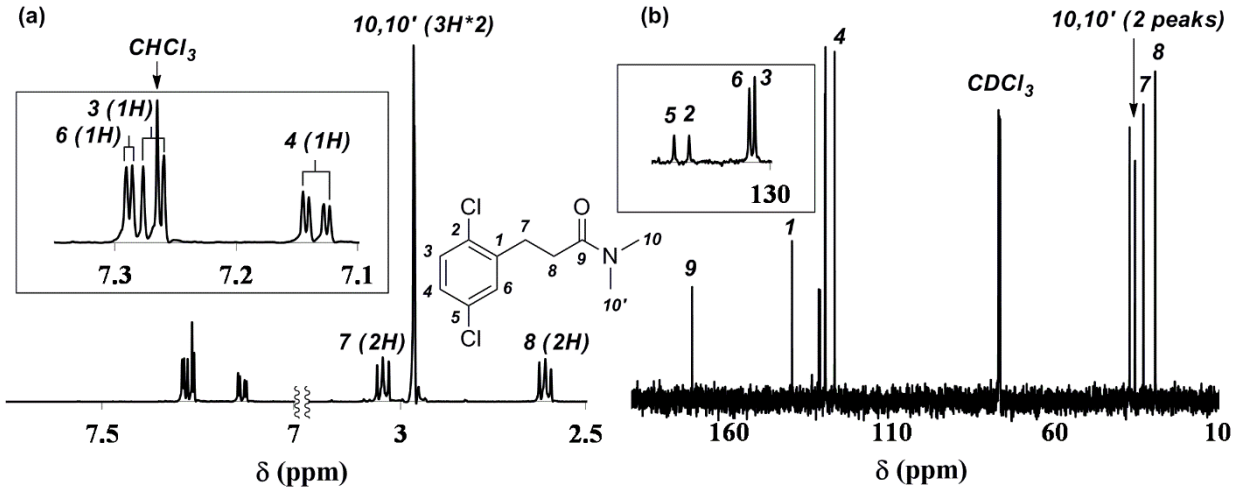

Figure S5. (a) ^{1}H and (b) ^{13}C NMR spectra of 3-(2,5-dichlorophenyl)-*N*,*N*-dimethylpropanamide (**4a**) in $CDCl_3$.

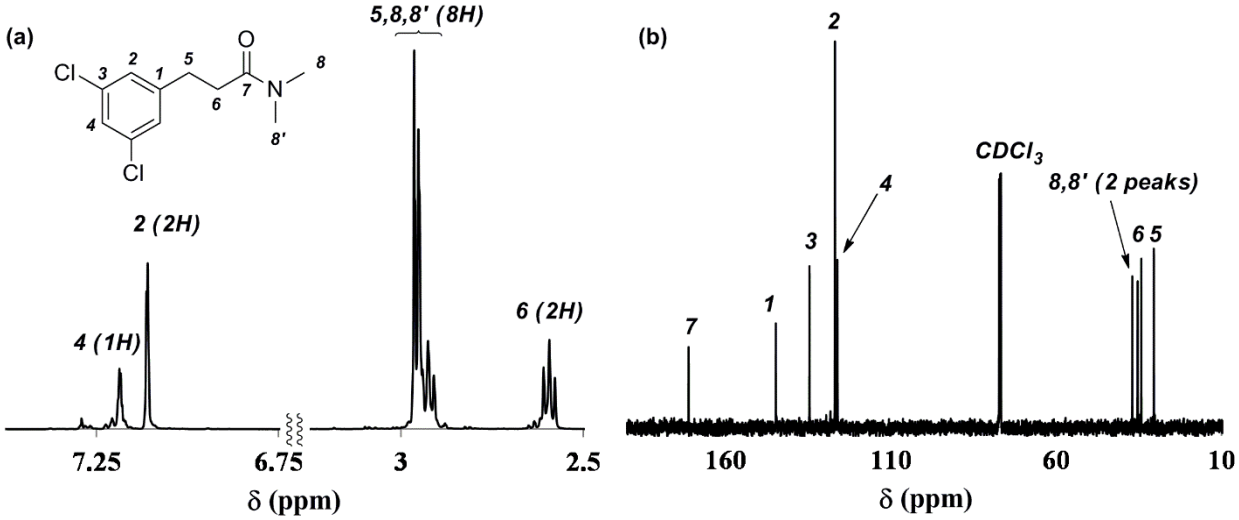

Figure S6. (a) ^{1}H and (b) ^{13}C NMR spectra of 3-(3,5-dichlorophenyl)-*N*,*N*-dimethylpropanamide (**4b**) in $CDCl_3$.

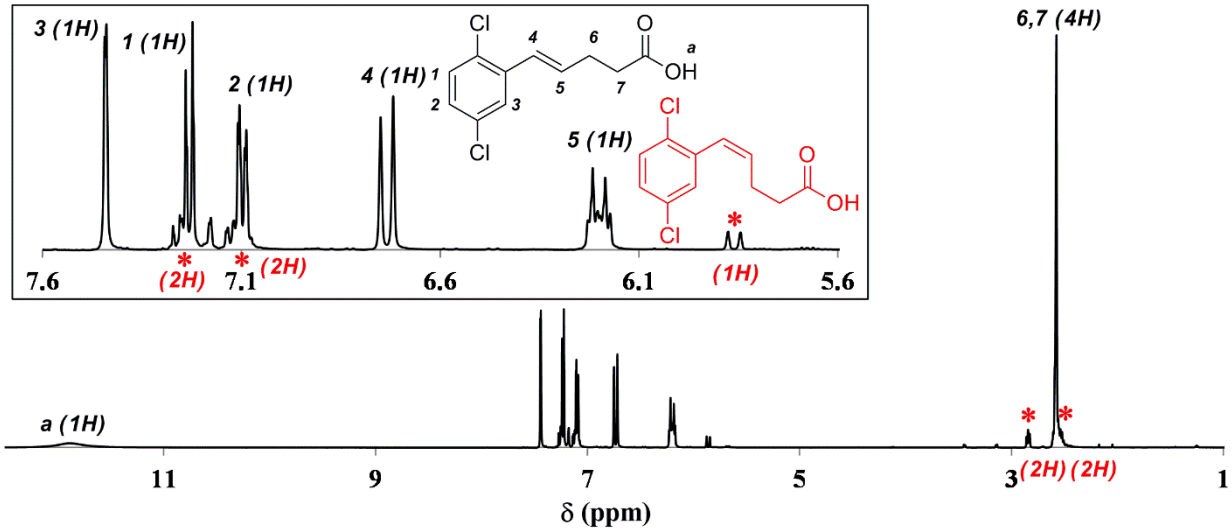

Figure S7. ^{1}H NMR spectrum of 5-(2,5-dichlorophenyl)-4-pentenoic acid (**6a**) in $CDCl_3$.

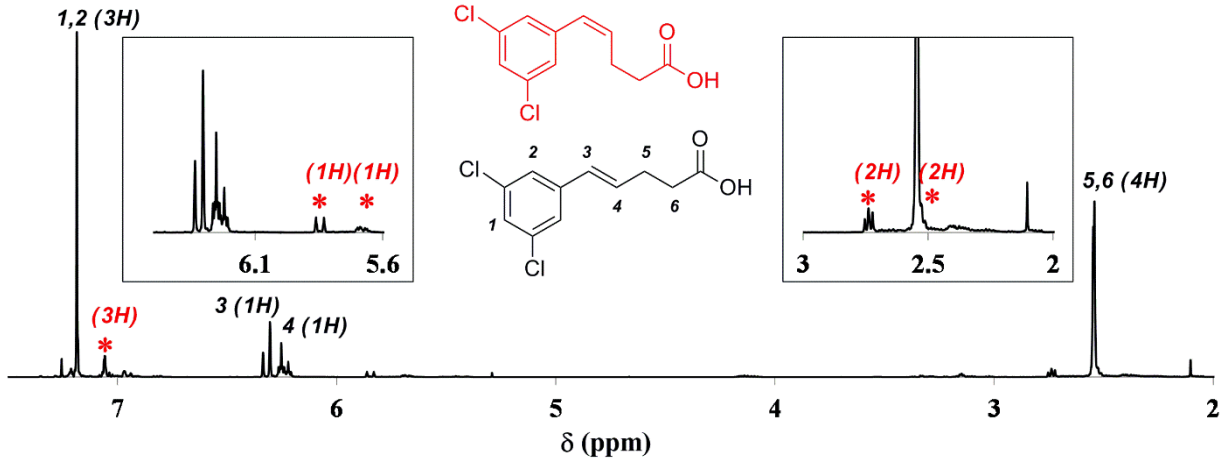

Figure S8. ^{1}H NMR spectrum of 5-(2,5-dichlorophenyl)-4-pentenoic acid (**6b**) in $CDCl_3$.

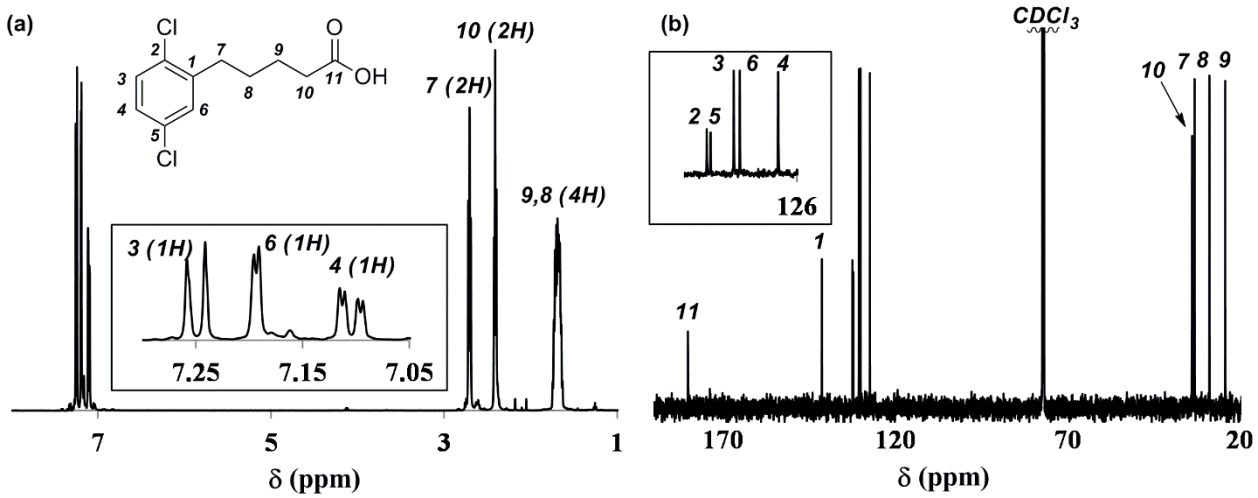

Figure S9. (a) ^{1}H and (b) ^{13}C NMR spectra of 5-(2,5-dichlorophenyl)pentanoic acid (**7a**) in $CDCl_3$.

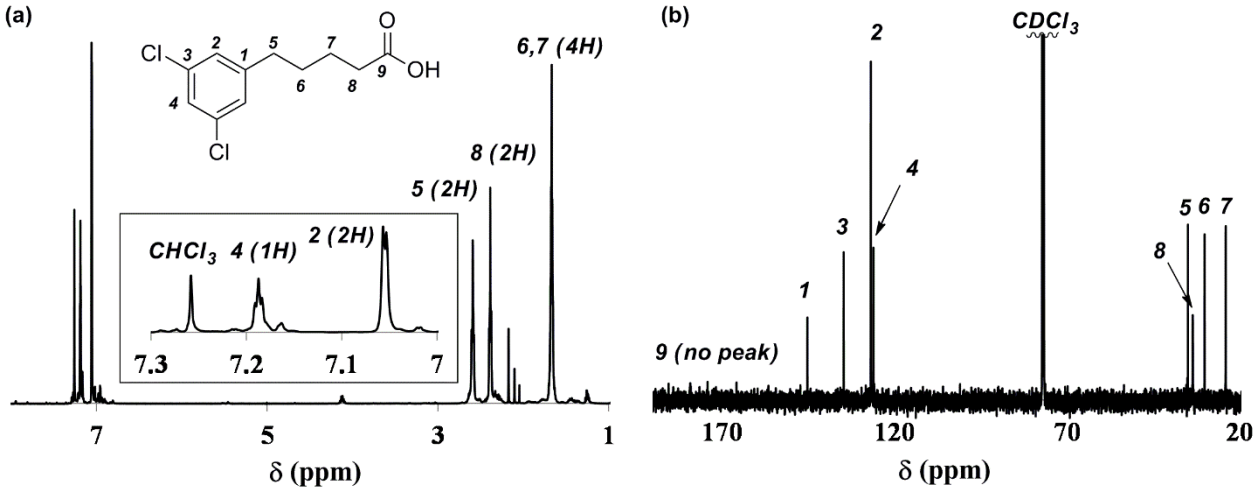

Figure S10. (a) ^{1}H and (b) ^{13}C NMR spectra of 5-(3,5-dichlorophenyl)pentanoic acid (**7b**) in $CDCl_3$.

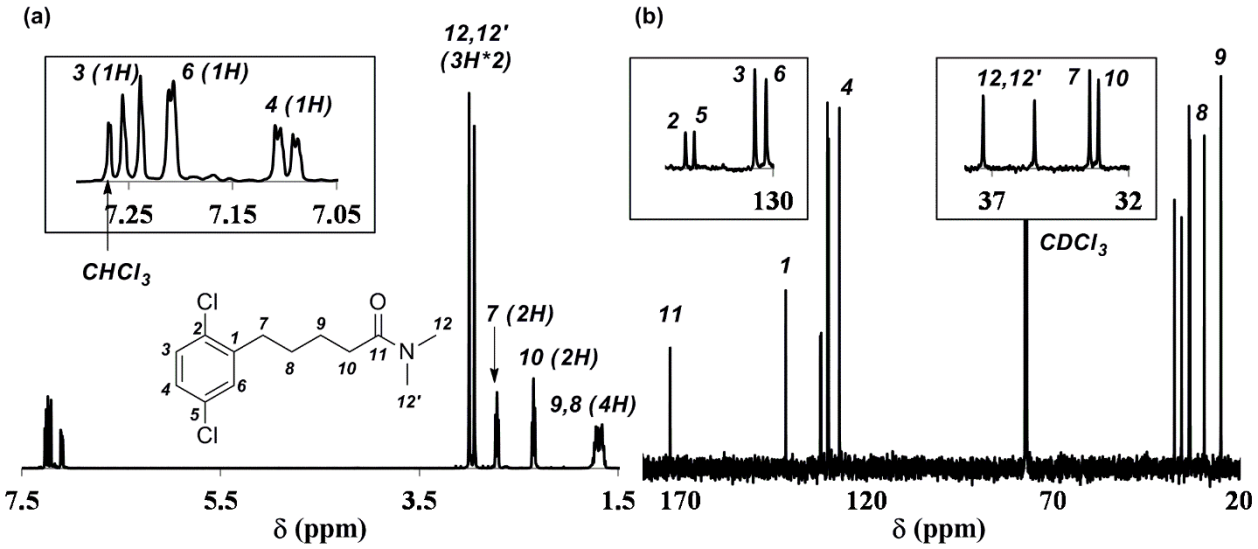

Figure S11. (a) ^{1}H and (b) ^{13}C NMR spectra of 5-(2,5-dichlorophenyl)-*N*,*N*-dimethylpentanamide (**8a**) in $CDCl_3$

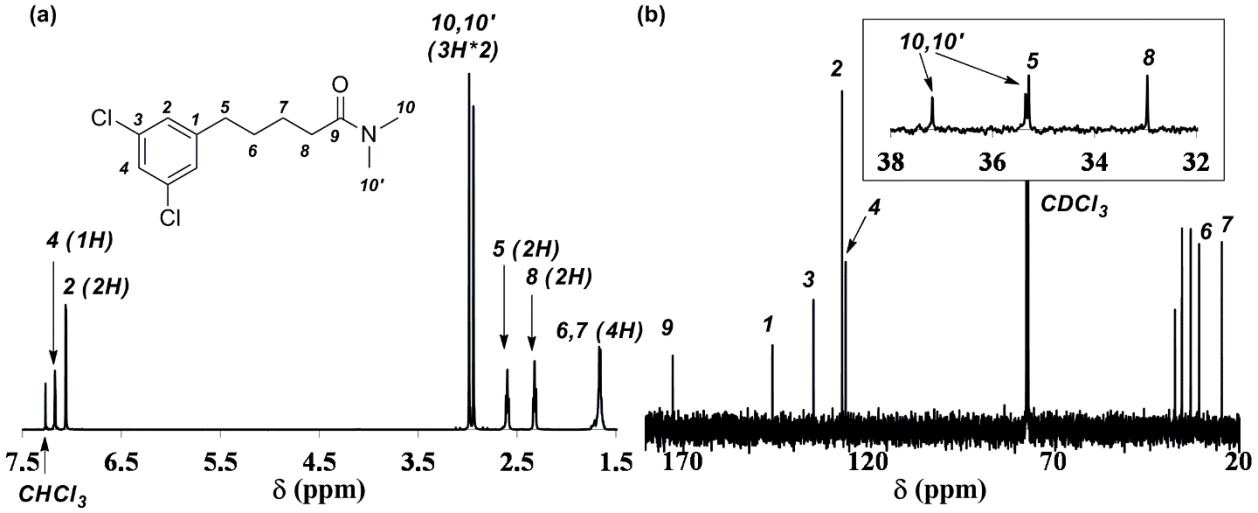

Figure S12. (a) ^{1}H and (b) ^{13}C NMR spectra of 5-(3,5-dichlorophenyl)-*N*,*N*-dimethylpentanamide (**8b**) in $CDCl_3$.

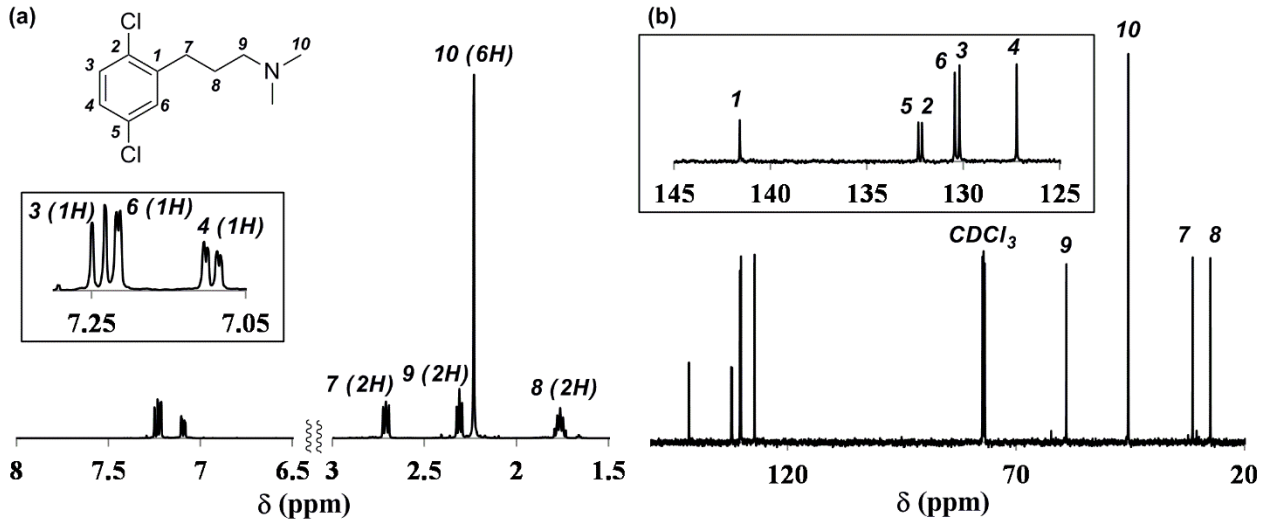

Figure S13. (a) ^{1}H and (b) ^{13}C NMR spectra of 3-(2,5-dichlorophenyl)-*N*,*N*-dimethylpropan-1-amine (**5a**) in $CDCl_3$.

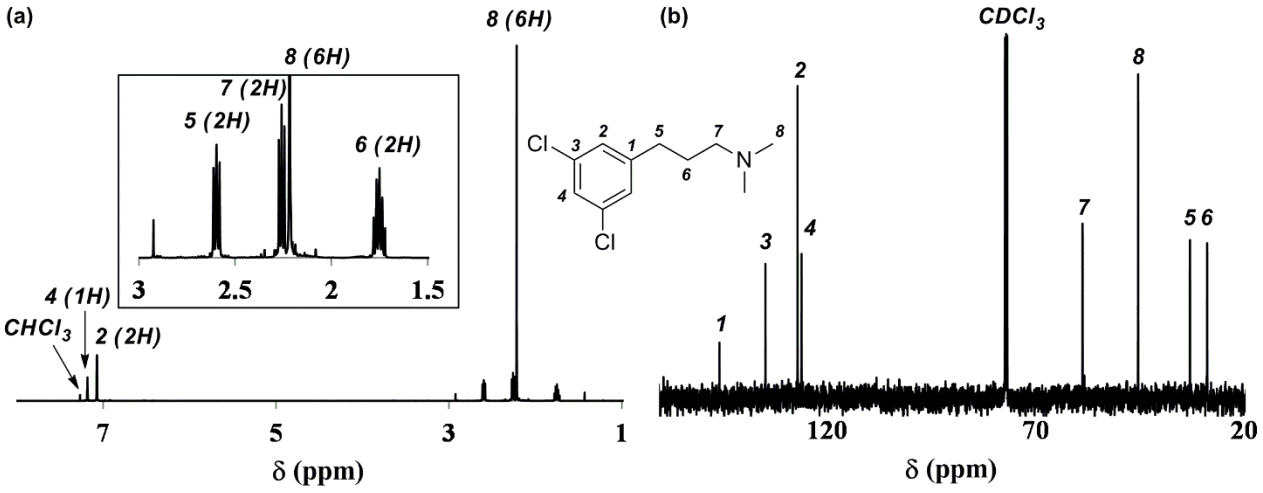

Figure S14. (a) ^{1}H and (b) ^{13}C NMR spectra of 3-(3,5-dichlorophenyl)-*N*,*N*-dimethylpropan-1-amine (**5b**) in $CDCl_3$

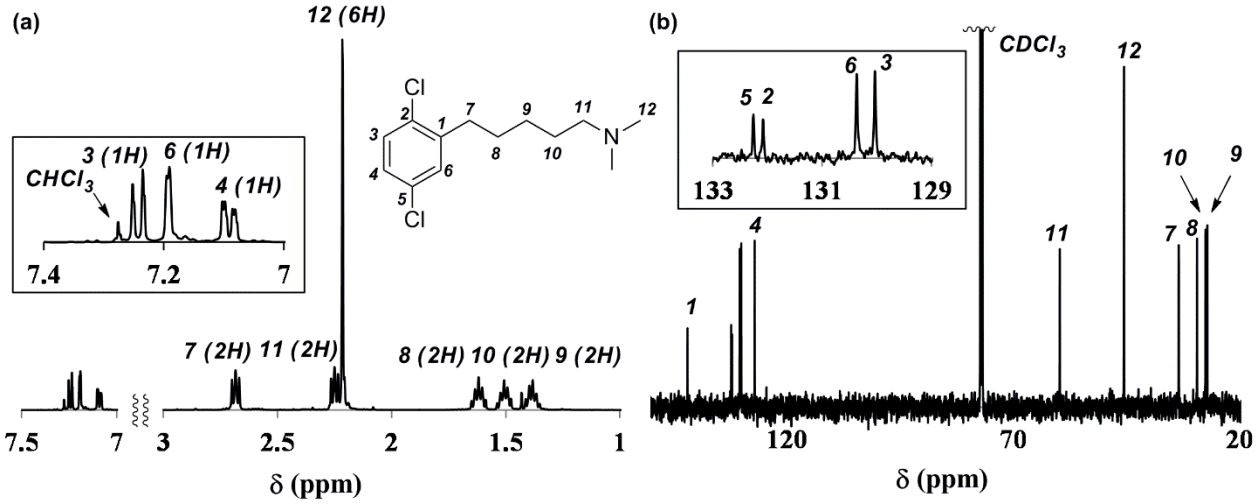

Figure S15. (a) ^{1}H and (b) ^{13}C NMR spectra of 5-(2,5-dichlorophenyl)-*N*,*N*-dimethylpentan-1-amine (**9a**) in $CDCl_3$.

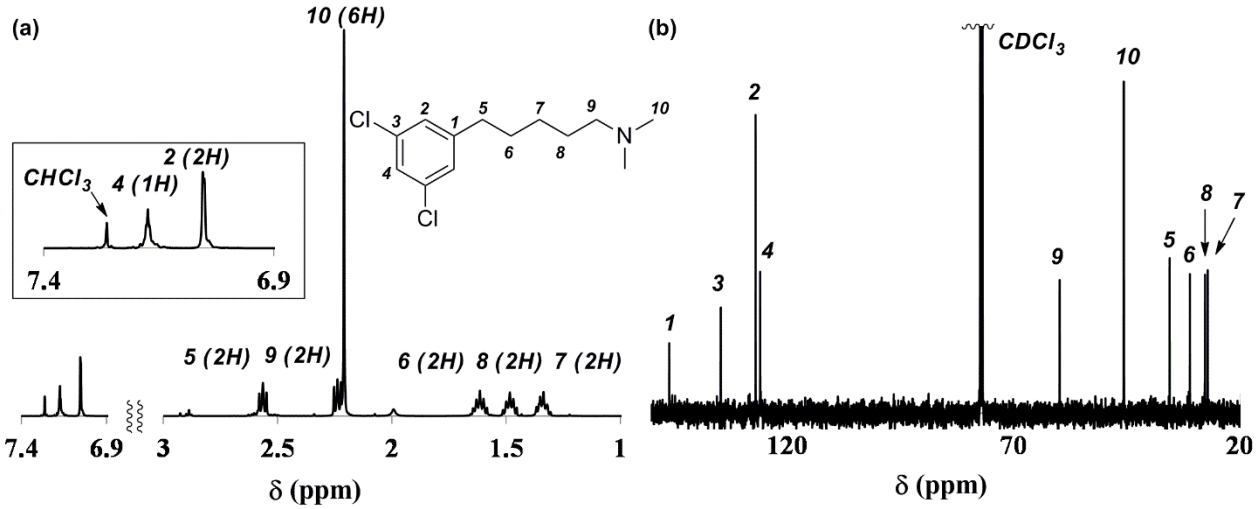

Figure S16. (a) ^{1}H and (b) ^{13}C NMR spectra of 5-(3,5-dichlorophenyl)-*N*,*N*-dimethylpentane-1-amine (**9b**) in $CDCl_3$.

Synthesis of QPE-*bl*-11s.

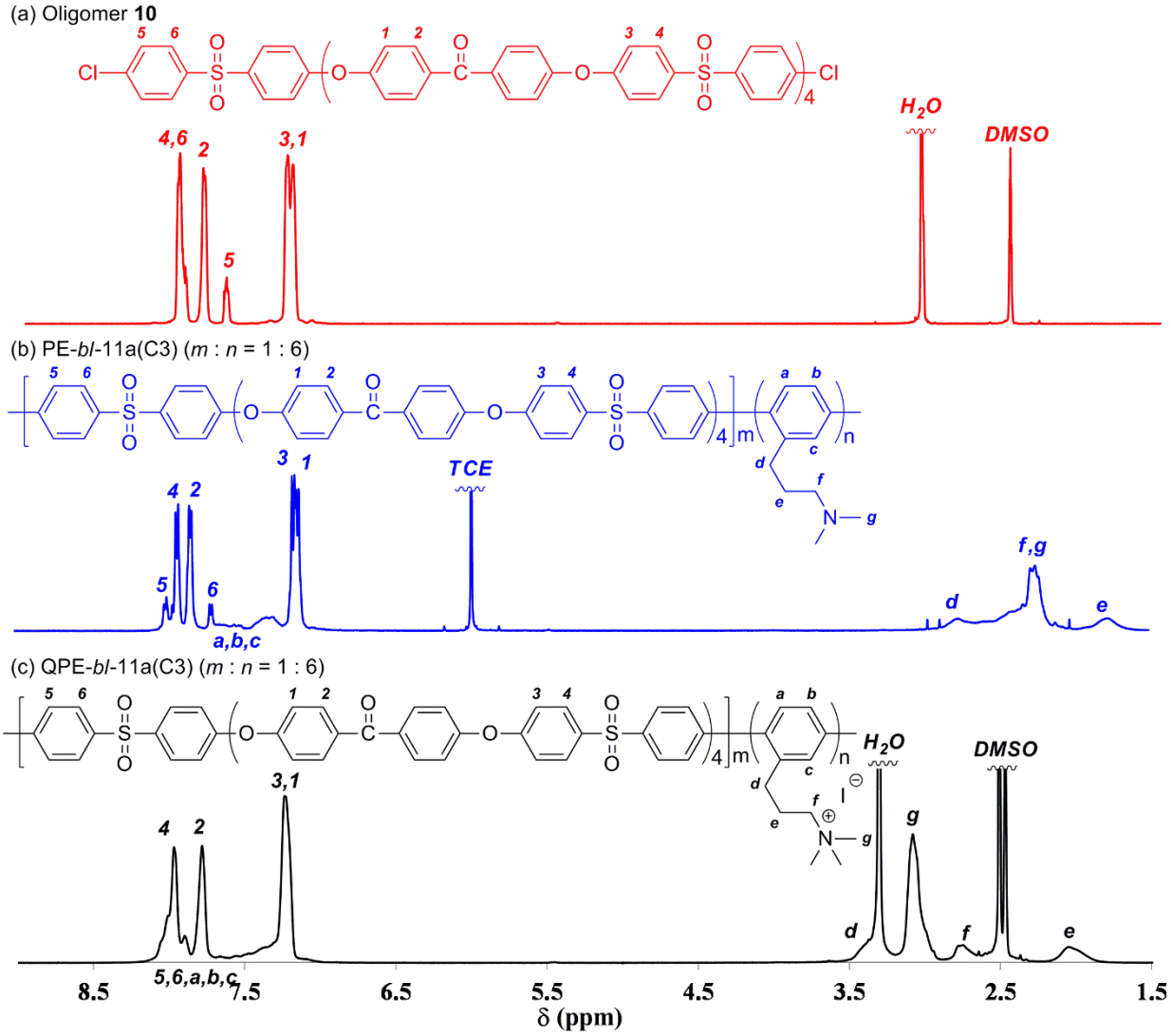

Figure S17. ^{1}H NMR spectra of (a) oligomer **10**, (b) PE-*bl*-11a(C3), and (c) QPE-*bl*-11a(C3) (*m* : *n* = 1 : 6).

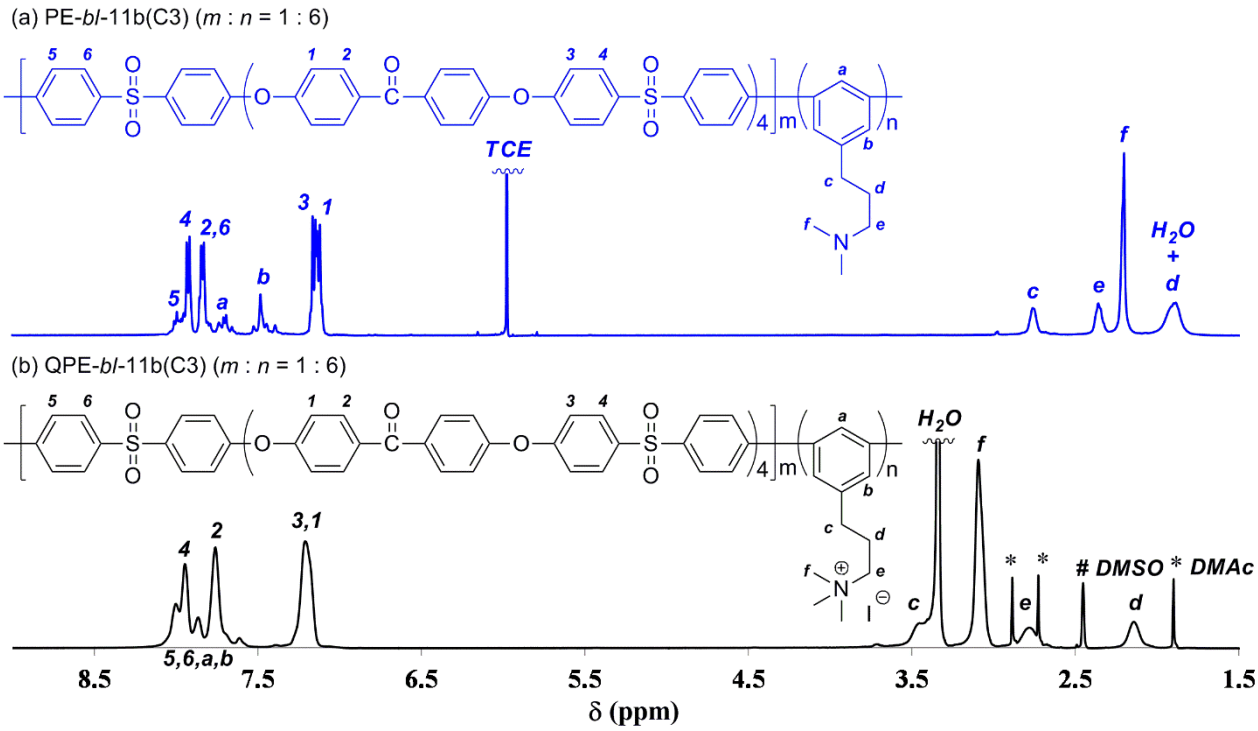

Figure S18. [1]H NMR spectra of (a) PE-*bl*-11b(C3) and (b) QPE-*bl*-11b(C3) (*m* : *n* = 1 : 6).

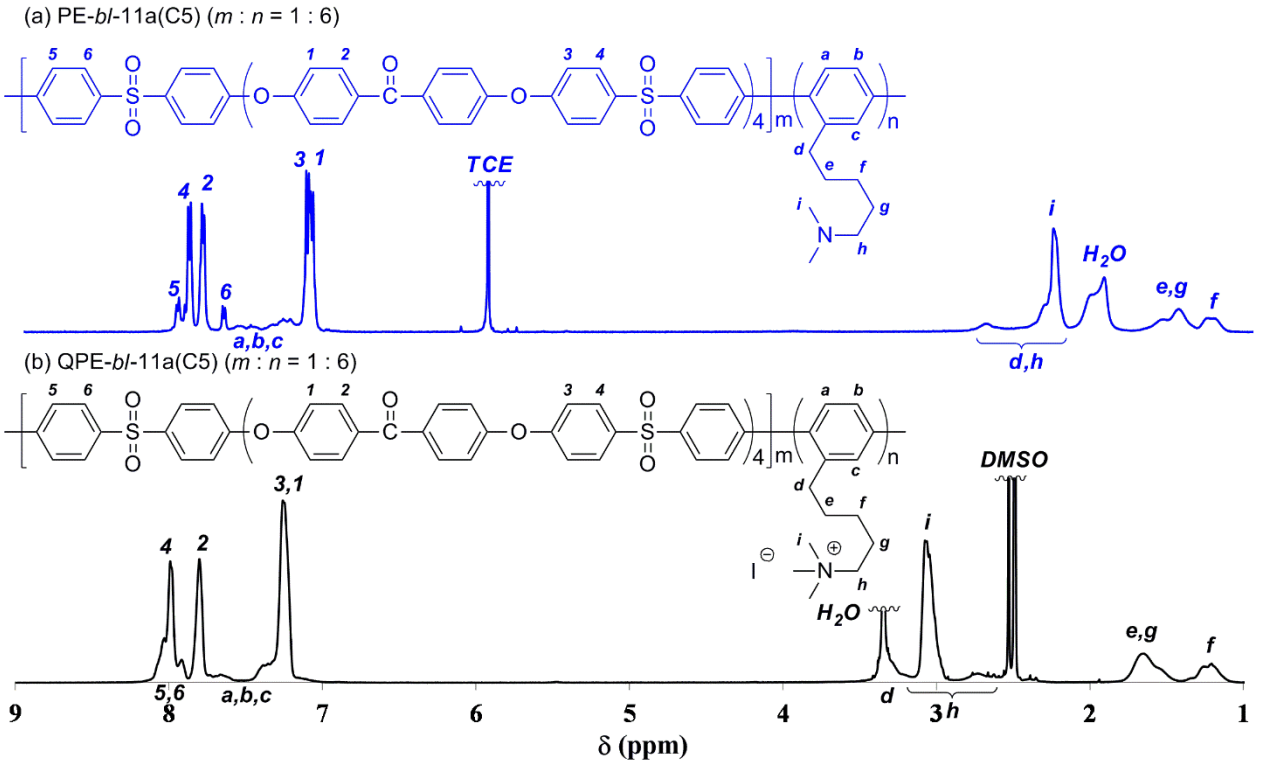

Figure S19. [1]H NMR spectra of (a) PE-*bl*-11a(C5) and (b) QPE-*bl*-11a(C5) (*m* : *n* = 1 : 6).

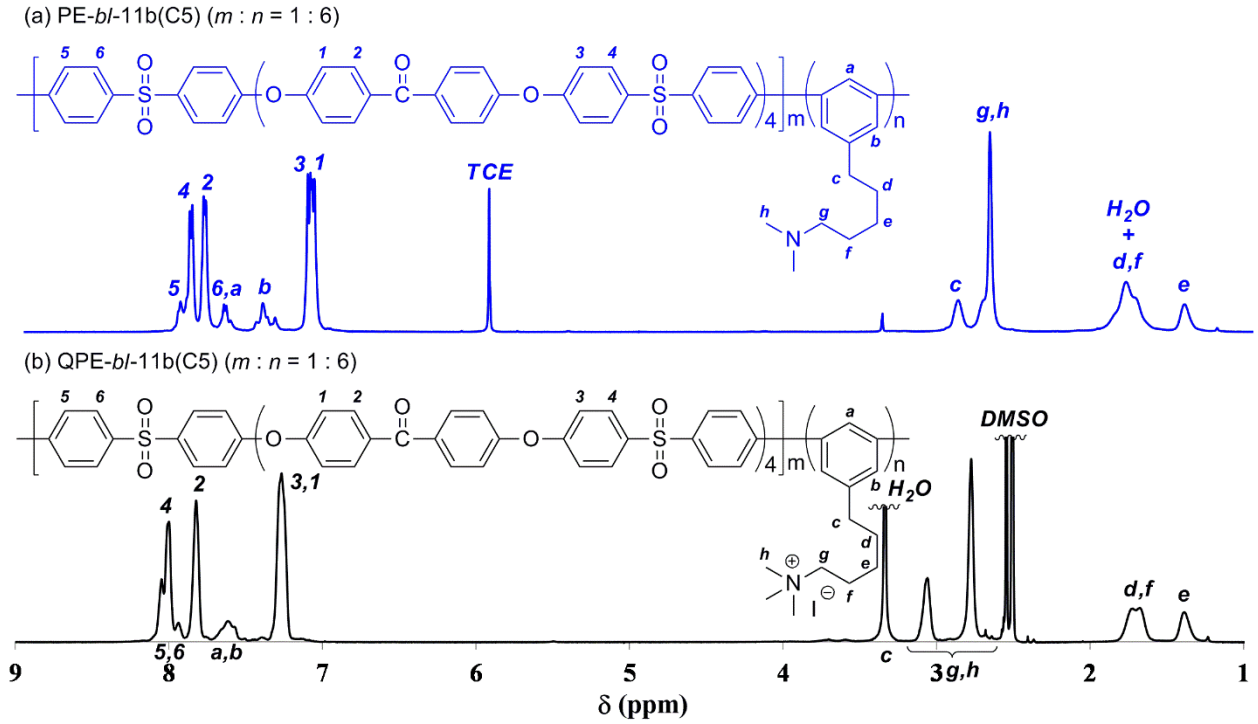

Figure S20. ^{1}H NMR spectra of (a) PE-*bl*-11b(C5) and (b) QPE-*bl*-11b(C5) (*m* : *n* = 1 : 6).

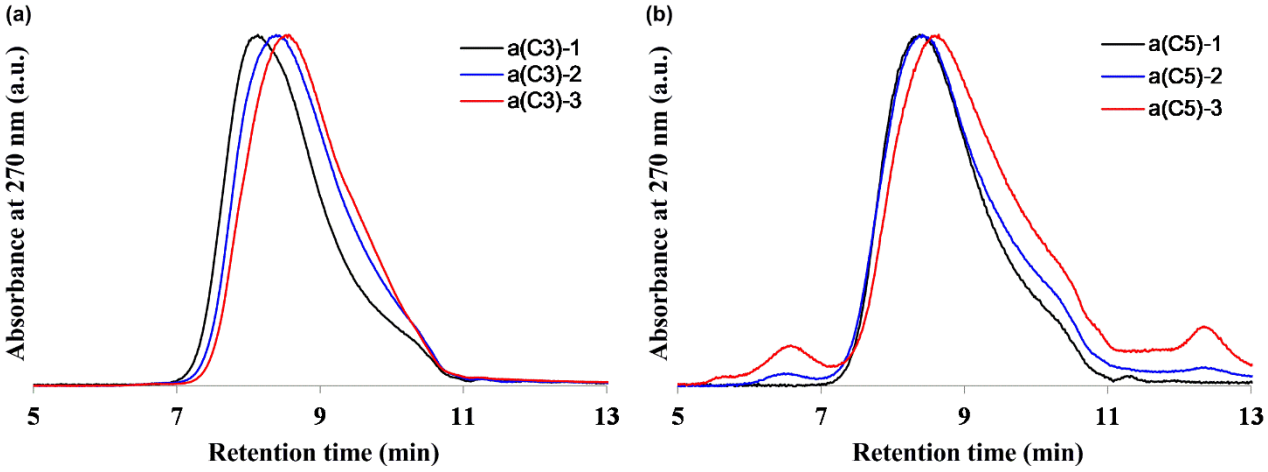

Figure S21. GPC profiles of (a) PE-*bl*-11a(C3) and (b) PE-*bl*-11a(C5).

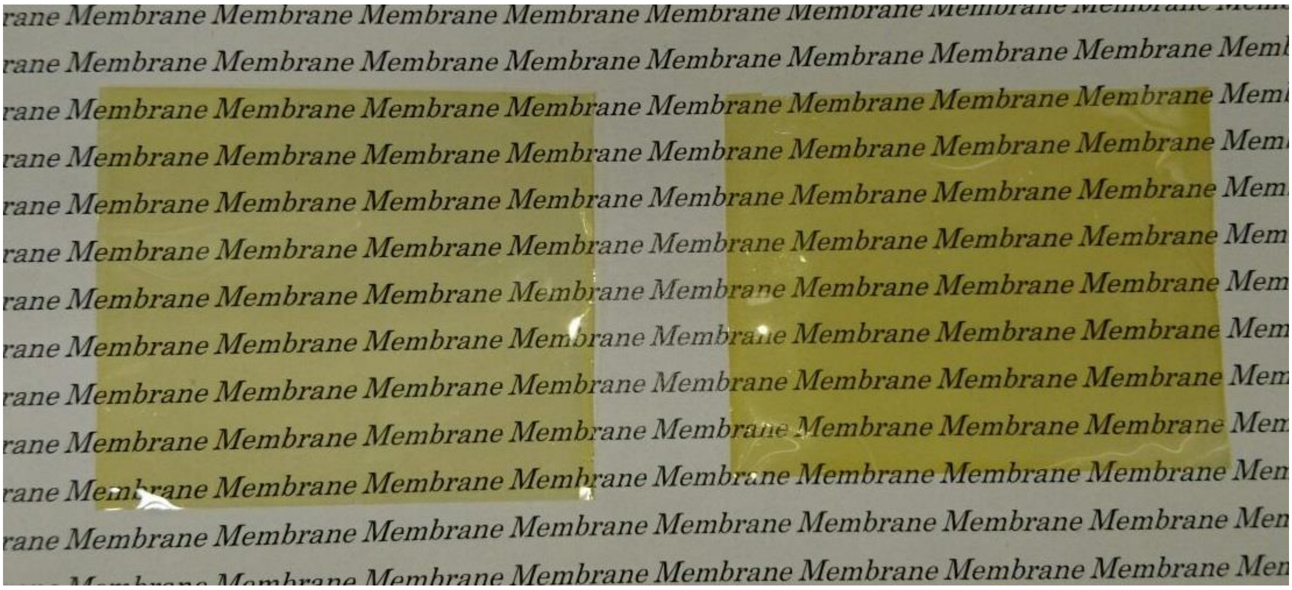

Figure S22. Photos of (left) QPE-*bl*-11a(C3) membrane (IEC = 1.92 mequiv g^{-1}) and (right) QPE-*bl*-11a(C5) membrane (IEC = 2.18 mequiv g^{-1}).

Morphology and Properties of QPE-*bl*-11 Membranes.

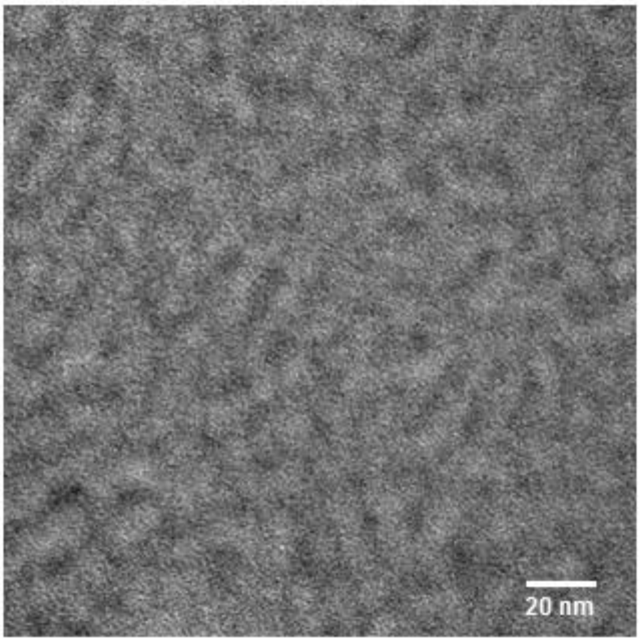

Figure S23. TEM image of QPE-*bl*-11a(C1) (IEC = 1.29 mequiv g^{-1}) membranes stained with tetrachloroplatinate ions.

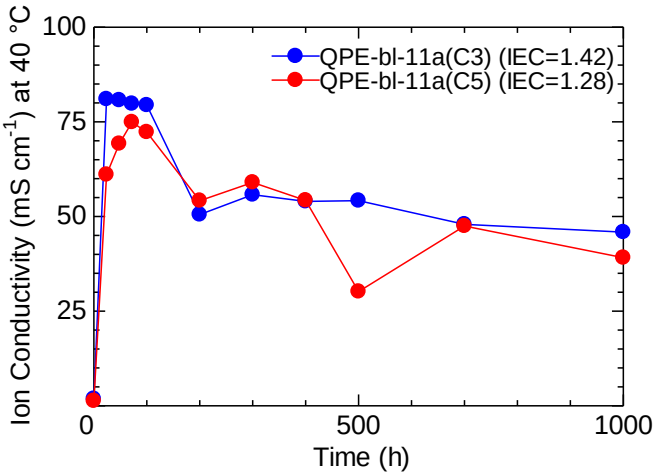

Figure S24. Time course of ion conductivity of QPE-*bl*-11a(C3), and -11a(C5) (IEC = 1.42 and 1.28 mequiv g^{-1}) membranes in 1 M KOH aqueous solution at 80 °C. The membranes were used in iodide ion forms to avoid the effect of carbon dioxide from the air.